ACS Catalysis

Research Article

pubs.acs.org/acscatalysis

In Situ Formation of Wilkinson-Type Hydroformylation Catalysts: Insights into the Structure, Stability, and Kinetics of Triphenylphosphine- and Xantphos-Modified Rh/SiO_2

Sankaranarayanapillai Shylesh, David Hanna, Anton Mlinar, Xüé-Qiān Kǒng, Jeffrey A. Reimer, and Alexis T. Bell*

Department of Chemical and Bimolecular Engineering University of California, Berkeley, Berkeley, California 94720, United States

Supporting Information

ABSTRACT: An investigation has been carried out to identify the effects of catalyst preparation on the activity, selectivity, and stability of phosphine-modified rhodium/silica catalysts (Rh/SiO_2) for propene hydroformylation. High selectivity to aldehydes was achieved, without the formation of propane or butanol. Catalyst activity and selectivity was found to depend strongly on the nature and concentration of the phosphine ligands and the amount of rhodium dispersed on the silica support. Screening of different ligands showed that a bidentate xantphos (X) ligand was ~2-fold more active than the monodentate phosphine ligand (PPh_3) screened at a ligand-to-rhodium ratio of 15:1. Investigation of the effects of reaction temperature, reactant partial pressures, and phosphine-to-rhodium ratio indicates that the kinetics of propene hydroformylation over X-promoted Rh/SiO_2 is nearly identical to those for sulfoxantphos-modified rhodium-containing supported ionic liquid phase (SX-Rh SILP) catalysts. In-situ FTIR and solid-state ^{31}P MAS NMR characterization provide evidence for the formation of $HRh(CO)_n(PPh_3)_{4-n}$ species on PPh_3-modified Rh/SiO_2, and $HRh(CO)_2(X)$ species on xantphos-modified Rh/SiO_2. The high catalytic activity observed over rhodium-containing silica catalysts is attributed to formation of $Rh^{(I)}(CO)_2$ species by the process of corrosive chemisorption of Rh nanoparticles by CO and the subsequent ligation of phosphine ligands to the dicarbonyl species. Evidence is also presented suggesting that the active form of the catalyst resides on the surface of the Rh nanoparticles.

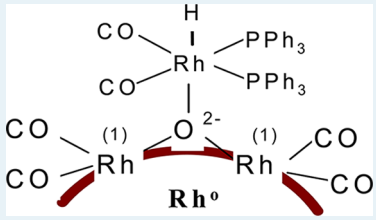

KEYWORDS: *rhodium, xantphos, phosphine ligands, butanal, hydroformylation*

1. INTRODUCTION

The hydroformylation of alkenes to produce aldehydes is carried out on a large scale using an aqueous solution of a Rh–tppts complex (tppts = tri(*m*-sulfonyl)triphenylphosphine trisodium salt).[1−3] Although this process is highly effective, it is limited to alkenes with fewer than four carbon atoms because of the low solubility of higher-molecular-weight alkenes. The need to separate the reaction products from the catalyst solution presents an additional challenge for carrying out alkene hydroformylation using homogeneous complexes.[4] Heterogenization of homogeneous catalysts on solid supports can easily mitigate these problems and enable alkene hydroformylation to be carried out in the gas phase or in the liquid phase without need for a solvent.[5,6] Several attempts have been made to achieve this goal. Davis and co-workers have shown that a supported aqueous phase catalyst can be prepared by dispersing tppts to $Rh(acac)(CO)_2$ dissolved in a thin aqueous layer within the pores of a high-surface-area silica.[7] Exposure of this impregnated solid to synthesis gas ($H_2/CO = 1$) at atmospheric pressure and room temperature produced an active catalyst for propene hydroformylation. Wasserscheid and co-workers have shown that supported ionic liquid phase (SILP) catalysts can be prepared by dispersing a solution of the catalyst complex in an ionic liquid (IL) as a thin film on the internal surface of a porous solid.[8−11] The advantage of using ILs over water is the near-zero vapor pressure of ILs, which virtually eliminates the loss of solvent under reaction conditions. Such SILP catalysts have been demonstrated to be highly effective for propene hydroformylation. The factors influencing the activity and stability of Rh-based SILP catalysts for the gas-phase hydroformylation of propene have been discussed by Shylesh et al.[12] Evidence from in situ FTIR and ^{31}P MAS NMR suggests that interactions of the IL and metal complex with the support are required to yield a stable catalyst. Catalyst activity is found to be a strong function of IL composition, as well as ligand-to-Rh ratio, IL loading, and temperature of support pretreatment. Ding and co-workers have reported a different approach for producing an active catalyst for propene hydroformylation. In this case, silica-supported Rh nanoparticles are promoted with PPh_3,[13,14] and Kim et al. have recently shown that the highest activity for PPh_3-modified Rh/SiO_2 is achieved for $PPh_3/Rh = 15$.[15] Because of the similarities in activation energies, partial and total pressure dependences of the reaction rates for PPh_3-modified Rh/SiO_2 and homogeneous $HRh(CO)(PPh_3)_3$ catalysts suggest that the active species in both systems are identical.

Received: November 16, 2012
Revised: January 14, 2013
Published: January 15, 2013

Here, we report the characterization and catalytic activity of a monodentate and bidentate phosphine-modified rhodium/silica (L-Rh/SiO_2, L = triphenylphosphine (PPh_3) and xantphos (X)) catalysts for the gas-phase hydroformylation of propene under mild reaction conditions. The objective of this work was to explore how the catalytically active species are formed under reaction conditions and the effects of how the ligand composition, the ligand/rhodium ratio, and rhodium loading affect the catalytic activity, selectivity, and stability of the L-Rh/SiO_2 catalyst relative to the silica-supported Wilkinson-type catalyst ($HRh(CO)(PPh_3)_3/SiO_2$). The kinetics of propene hydroformylation on bidentate xantphos-modified Rh/SiO_2 catalyst (X-Rh/SiO_2) and PPh_3-modified Rh/SiO_2 catalyst (PPh_3-Rh/SiO_2) are also discussed. In situ FTIR characterization of the phosphine-modified Rh/SiO_2 catalyst was performed to obtain evidence for the formation of active species under the reaction conditions. These observations were complemented by ex-situ characterization of the catalysts by ^{31}P MAS NMR and HR-TEM. Results of the present study provide additional experimental evidence for in situ formation of homogeneous catalysts and the interactions of the homogeneous catalyst with the rhodium nanoparticles dispersed on the support surfaces.

2. EXPERIMENTAL SECTION

The preparation of PPh_3-modified Rh/SiO_2 was as follows: 0.2 wt % Rh/SiO_2 was prepared by incipient-wetness impregnation of mesoporous SiO_2 (Silicycle, 500 m^2 g^{-1}, average pore diameter 60 Å) with a solution of rhodium(III) acetyl acetonate (Aldrich, 97% pure) dissolved in toluene (Alfa Aesar, anhydrous 99.8% pure). After impregnation, the solid was dried at 393 K for 12 h, then calcined in 100 cm^3 min^{-1} 10% O_2/He (Praxair, certified standard) for 4 h at 673 K (2 K min^{-1}) and, finally, reduced in 100 cm^3 min^{-1} 9% H_2/He (Praxair, certified standard) at 673 K for 4 h. Using incipient-wetness impregnation, a solution of PPh_3 (Aldrich, 99% purity) in toluene was absorbed onto the SiO_2-supported Rh under nitrogen atmosphere. After the impregnation, the solid was dried for 2 h at ambient temperature in nitrogen and then dried in a vacuum oven at 353 K for 12 h. The PPh_3/toluene solution concentration was varied to obtain final molar ratios of PPh_3/Rh between 5 and 20, and the rhodium loading was varied from 0.05 to 1 wt %. A similar incipient-wetness impregnation procedure using toluene as a solvent was used for the preparation of xantphos-modified Rh/SiO_2 catalysts (X-Rh/SiO_2).

Gas-phase hydroformylation of propene was performed in a 6.35 mm o.d. (~4 mm ID) quartz tube containing an expanded section (~12.7 mm o.d., ~20 mm length). The reactor was packed with quartz wool above and below the catalyst bed to hold the catalyst in place. The feed to the reactor consisted of propene (Praxair, 3.0 grade), CO (Praxair, 4.0 research grade), and H_2 (Praxair, 5.0 UHP grade). A reactant ratio of C_3H_6/CO/H_2 of 1:1:1 was used unless specified otherwise. Experiments were carried out at 393 K, total gas pressures of 2 atm, and total gas flow rate of 120 cm^3 min^{-1} at STP to maintain a constant volumetric flow rate of 60 cm^3 min^{-1} at pressure. Under these conditions, the conversion of propene was always <1%. Reaction products were analyzed using an Agilent 6890N gas chromatograph containing a bonded and cross-linked (5% phenyl)-methylpolysiloxane capillary column (Agilent, HP-1) connected to a flame ionization detector.

Infrared spectra were acquired using a Thermo Scientific Nicolet 6700 FTIR spectrometer equipped with a liquid-nitrogen-cooled MCT detector. Each spectrum was obtained by averaging 32 scans taken with 1 cm^{-1} resolution. For IR studies, 0.05 g of the catalyst was pressed into a 20-mm-diameter pellet (<1 mm thick) and placed into a custom-built transmission cell equipped with CaF_2 windows, a K-type thermocouple for temperature measurement, and resistive cartridge heaters. All scans were acquired at 393 K. Experiments at elevated pressure were carried out by throttling a needle valve located downstream from the reactor. Pure CO was passed through a trap packed with 3.2 mm pellets of 3 Å molecular sieve to remove iron pentacarbonyl formed within the cylinder.

Solid-state ^{31}P MAS NMR experiments were performed on a Bruker Avance I-500 MHz spectrometer using a frequency of 202.5 MHz, 90° pulse in 4.2 μs, and a delay of 60 s relative to 85% H_3PO_4. High-resolution transmission electron microscopy (HR-TEM) characterizations were conducted on the TEAM 0.5 high-resolution electron microscope, a modified FEI Titan 80-300 TEM equipped with a gun monochromator, operated at 80 KV at the National Center for Electron Microscopy (NCEM). Scanning transmission electron microscopy (STEM) images were taken on a FEI Tecnai F20 microscope operated at 200 KV and incorporated with a gun monochromator.

3. RESULTS

3.1. Catalytic Activity of Phosphine-Modified Rh/SiO_2 Catalysts. *3.1.1. Effect of Ligand Composition.* It is known that the activity, selectivity, and stability of homogeneous rhodium−phosphine complexes used for hydroformylation reactions are sensitive to the structure and concentration of the ligand.[1] The role of various phosphine ligands was therefore investigated at a fixed ligand-to-rhodium molar ratio of 15 (L/Rh = 15) and a rhodium loading of 0.2 wt %. The ligands screened include triphenylphosphine (PPh_3), triphenyl phosphite ($P(OPh)_3$), fluorinated triphenylphosphine (3F-PPh_3), methoxytriphenylphosphine (OMe-PPh_3), and bidentate xantphos (X). Table 1 shows that ligand composition had a strong effect on the catalyst activity and n/iso ratio. Under identical reaction conditions, Rh/SiO_2 modified by bidentate xantphos was ~2-fold more active than the Rh/SiO_2 modified by monodentate phosphine ligands. The catalytic activity and n/iso ratio observed for X-Rh/SiO_2 catalyst were similar to that observed over sulfoxantphos-containing Rh-SILP (supported ionic liquid phase) catalysts[12] (see Supporting Information).

Table 1. The Effects of Phosphine Composition on the Rate of Propene Hydroformylation and the n/iso Ratio of Butanals Formed on Phophine-Modified Rh/SiO_2[a]

catalyst	L/Rh ratio[b]	rate (h^{-1})[c]	n/iso[d]
X-Rh/SiO_2	15	78	13
PPh_3-Rh/SiO_2	15	35	9
3F-PPh_3-Rh/SiO_2	15	31	12
OMe-PPh_3-Rh/SiO_2	15	15	8
$P(OPh)_3$-Rh/SiO_2	15	24	3
SX-Rh/SILP	15	83	13

[a]Reaction conditions: $C_3H_6/H_2/CO$ = 1:1:1, P_{total} = 2 atm, T = 393 K, t = 8 h, 0.2 wt % Rh metal loading. [b]Molar ligand-to-metal ratio. [c]Turnover frequency in moles of aldehyde per mole of Rh per hour. [d]Linear-to-branched ratio.

dx.doi.org/10.1021/cs3007445 | ACS Catal. 2013, 3, 348−357

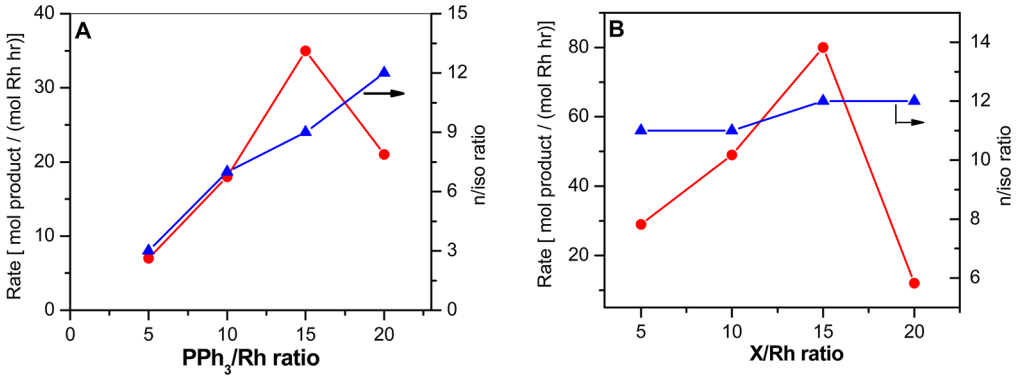

Figure 1. The effect of (A) PPh_3/Rh and (B) X/Rh ratios on the rates of butanal synthesis. P_{total} = 2 atm; $P_{C_3H_6}/P_{CO}/P_{H_2}$ = 1:1:1; T = 393 K; L/Rh molar ratio = 5−20; Rh = 0.2 wt %; catalyst mass = 0.3 g; total gas flow rate = 60 cm^3 min^{-1} at pressure, 120 cm^3 min^{-1} at STP.

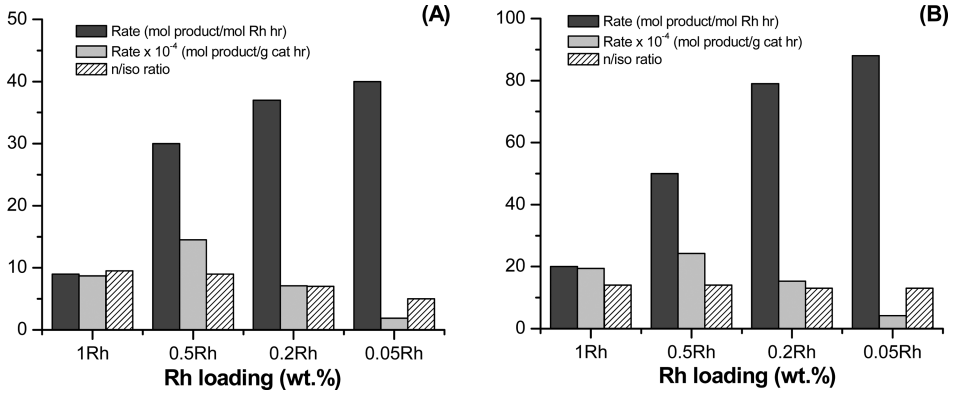

Figure 2. The effect of rhodium loading on the rates of butanal synthesis: (A) PPh_3 ligand and (B) Xantphos ligand. P_{total} = 2 atm; $P_{C_3H_6}/P_{CO}/P_{H_2}$ = 1:1:1; T = 393 K; L/Rh molar ratio = 15; total gas flow rate = 60 cm^3 min^{-1} at pressure, 120 cm^3 min^{-1} at STP.

The higher activity of Rh complexes involving xantphos over monodentate phosphines can be attributed to the chelating ability of xantphos, which yields a higher concentration of the coordinated rhodium species.[1] Quite interestingly, an n/iso ratio of 3 was observed over the phosphite-modified Rh/SiO_2 catalysts. Use of derivatives of triphenylphosphine with substituents typically in the para positions can obviate the problems of simultaneously changing the electronic and steric features of phosphine ligands.[16] For instance, electron-withdrawing groups in the para position decrease the basicity of the triphenylphosphine groups, whereas electron-donating groups decrease the electrophilicity over the rhodium center without altering the steric confinement around the rhodium site. Accordingly, it should be noted that the n/iso ratio of the aldehyde increased as the electron density around the rhodium was decreased by using electron-withdrawing substituents in the modifying phosphine ligand (-F vs -OMe, Table 1). In other words, less basic triaryl phosphines enhance the formation of linear products, whereas the more basic triaryl phosphine groups lead to lower n/iso ratios.

3.1.2. Effect of L/Rh Molar Ratio. To investigate the role of phosphine ligands on the catalytic performance of Rh/SiO_2 catalysts, the L/Rh molar ratio (L = PPh_3 and X) was varied from 5 to 20 at a fixed rhodium loading of 0.2 wt %. In the absence of ligands, Rh/SiO_2 is inactive for hydroformylation, clearly showing the importance of phosphine ligands for promoting hydroformylation. Neither propane nor butanol was observed in the reaction products, indicating that the phosphine-modified Rh/SiO_2 catalysts are highly selective toward the formation of aldehydes. The results in Figure 1 show that the hydroformylation rate increased rapidly with increasing L/Rh ratio up to a molar ratio of 15, and above this value, the activity toward both products declined. The observed patterns were qualitatively similar for PPh_3 and X, but the catalytic activity was roughly 2-fold higher for X. Irrespective of the L/Rh composition, bidentate xantphos-modified Rh/SiO_2 exhibited an almost constant n/iso ratio of 12. It is important to note that an optimal X/Rh ratio has also been reported in studies of $HRh(CO)_2(X)$ complexes dissolved in various solvents.[17,18] By contrast, for PPh_3-modified Rh/SiO_2, the rate of linear product formation grew more rapidly than the rate of branched product formation up to a PPh_3/Rh ratio of 20, increasing the n/iso ratio from ∼3 to 13 (Figure 1A). The high n/iso ratio observed in the present study for $PPh_3/Rh \geq 15$ is consistent with studies conducted with $HRh(CO)(PPh_3)_3$ in homogeneous solutions.[15]

3.1.3. Effect of Rhodium Loading. The role of rhodium loading on the phosphine-modified Rh/SiO_2 catalyst was investigated by varying the rhodium concentration on the silica support from 0.05 to 1 wt % at a fixed L/Rh molar ratio of 15. Figure 2 shows that, irrespective of ligand composition, the rate per rhodium atom increased almost 4-fold as the loading of rhodium decreased from 1 to 0.05 wt %. It was also found that the n/iso ratio decreased from ∼9 to 4 with a decrease in the rhodium weight loading with the PPh_3-modified Rh/SiO_2 catalysts, whereas the n/iso ratio remained constant at ∼13 for the bidentate xantphos-modified Rh/SiO_2 catalysts.

dx.doi.org/10.1021/cs3007445 | ACS Catal. 2013, 3, 348−357

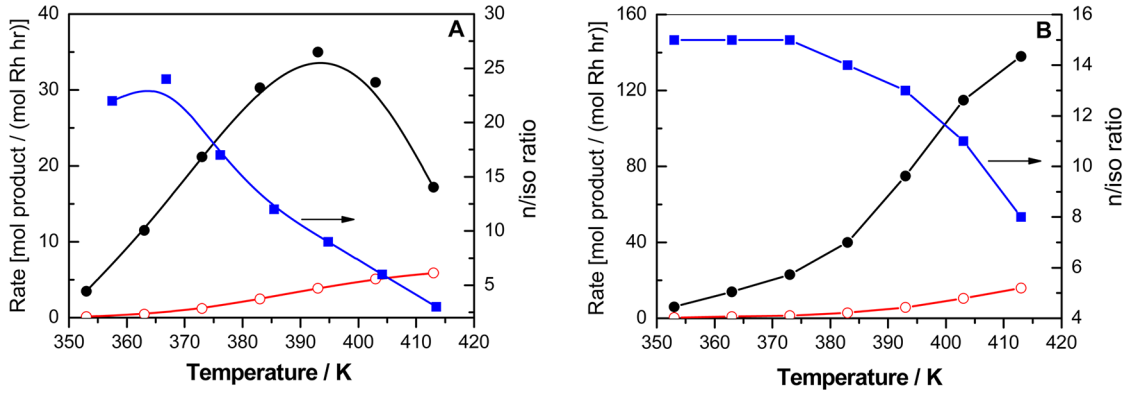

Figure 3. Effect of temperature on the rate of butanal synthesis and regioselectivity over (A) PPh_3-Rh/SiO_2 and (B) X-Rh/SiO_2 catalysts. P_{total} = 2 atm; $P_{C_3H_6}/P_{CO}$:P_{H_2} = 1:1:1; catalyst mass = 0.3 g; X/Rh molar ratio = 15; Rh = 0.2 wt %; total gas flow rate = 60 cm^3 min^{-1} at pressure, 120 cm^3 min^{-1} at STP (black line represents *n*-butanal and red line represents *i*-butanal).

3.2. Kinetics of Propene Hydroformylation Using L-Rh/SiO_2 Catalysts. Time-on-stream studies demonstrated that the L-Rh/SiO_2 catalysts were stable for 30 h, and no deactivation was observed under the reaction conditions (see Supporting Information). There is no loss in the rhodium content on phosphine-modified Rh/SiO_2 catalysts as analyzed from the ICP-OES analysis. The only products observed under any of the conditions investigated were *n*- and isobutanal. Figure 3 shows the effects of reaction temperature on the catalytic activity and the n/iso ratio of the phosphine-modified Rh/SiO_2 catalyst (PPh_3-Rh/SiO_2) and xantphos-modified Rh/SiO_2 catalyst (X-Rh/SiO_2) for a L/Rh molar ratio of 15. For PPh_3-Rh/SiO_2 catalysts, the rate of *n*-butanal formation increased with temperature up to 393 K, after which the rate decreased. The ratio of *n*- to isobutanal reached a maximum value of 24 at 363 K and then decreased sharply to 3 at 413 K. The decrease in the rate of *n*-butanal formation above 393 K is attributable to decomposition of PPh_3, which is confirmed by TGA analysis (see Supporting Information). For X-Rh/SiO_2 catalysts, the rates of *n*- and isobutanal formation increased as the reaction temperature increased. At 403 K, the rate of *n*-butanal formation begins to plateau while the rate of isobutanal formation continues to rise. Thus, the n/iso ratio decreases from 15 at 353 K to 8 at 413 K, demonstrating that temperature can be used to control the n/iso ratio. Above 413 K, a loss in catalytic activity due to ligand decomposition was noted, as identified by thermal gravimetric analysis.

The apparent activation energies calculated from the Arrhenius plot for PPh_3-Rh/SiO_2 in the temperature interval 353−413 K are 65 and 56 kJ mol^{-1}, respectively (Table 2). For X-Rh/SiO_2, the apparent activation energy measured over the interval 353−413 K for *n*-butanal formation is 65 kJ mol^{-1}, whereas the apparent activation energy for isobutanal formation is 75 kJ mol^{-1}. These values are ∼5 kJ mol^{-1} higher than those previously reported for a sulfoxantphos ligand containing Rh-SILP catalysts.[19]

The dependences of the rate of *n*- and isobutanal formation on the partial pressures of propene, CO, and H_2 were measured by holding the partial pressures of two components at 0.67 atm while varying the partial pressures of the third reactant and He. The total gas flow rate and pressure were kept constant at 60 cm^3 min^{-1} and 2 atm (120 cm^3 min^{-1} at STP). Table 3 shows the effect of varying the partial pressures of C_3H_6, CO, and H_2 partial pressures on the catalytic activity at 363 K of phosphine ligand-modified Rh/SiO_2 catalysts and a sulfoxantphos-containing Rh-SILP catalyst. As shown in Table 3, for X-Rh/SiO_2, the partial pressure dependence of H_2 on the rate of *n*-butanal formation is 0.12, the partial pressure dependence on CO is −0.47, and the partial pressure dependence on C_3H_6 is 0.86. The orders of reaction with respect to the partial pressures of H_2, CO, and C_3H_6 for *n*- and isobutanal formation are similar. The partial pressure dependences observed for X-Rh/SiO_2 are similar to those observed for the sulfoxantphos-containing Rh-SILP catalysts (Table 3). By contrast, a first-order dependence in C_3H_6, CO, and H_2 was noted with the phosphine-modified PPh_3-Rh/SiO_2 catalysts.[15]

Table 2. Comparison of Activation Energies for the Formation of n- and Isobutanal over Different Phosphine-Containing Rhodium Catalysts

catalyst	reaction phase	E_A (kJ/mol)	temp (K)	pressure (atm)	ref
X-Rh/SiO_2	gas	65.0[a]	353−373	2	this work
		75.0[b]			
PPh_3-Rh/SiO_2	gas	65.0[a]	353−373	2	15
		57.0[b]			
SX-Rh-SILP	gas	60.0[a]	353−373	2	19
		72.0[b]			

[a]*n*-Butanal. [b]Isobutanal.

Table 3. Apprent Reaction Order in Propene, CO, and H_2 over Phosphine-Modified Rh/SiO_2 Catalysts[a]

	reactant		
catalyst	C_3H_6	CO	H_2
X-Rh/SiO_2	0.86[b]	−0.47	0.12
	0.76[c]	−0.40	0.12
PPh_3-Rh/SiO_2	1.01[b]	1.12	1.02
	0.99[c]	0.90	0.85
SX-Rh- SILP	0.93[b]	−0.43	0.10
	0.92[c]	−0.61	0.00

[a]Error bars were ∼±3 for all the numbers. [b]*n*-Butanal. [c]Isobutanal.

3.3. Characterization of Phosphine-Modified Rh/SiO_2 Catalysts. *3.3.1. In Situ FTIR.* In situ FTIR was used to identify how the phosphine-modified Rh/SiO_2 (L-Rh/SiO_2, L = PPh_3 and X) changed upon exposure to CO and then CO/H_2. At very low CO partial pressure (0.2 atm), the IR spectra of PPh_3-modified 1%Rh/SiO_2 (PPh_3/Rh = 15) showed a sharp band at

dx.doi.org/10.1021/cs3007445 | ACS Catal. 2013, 3, 348−357

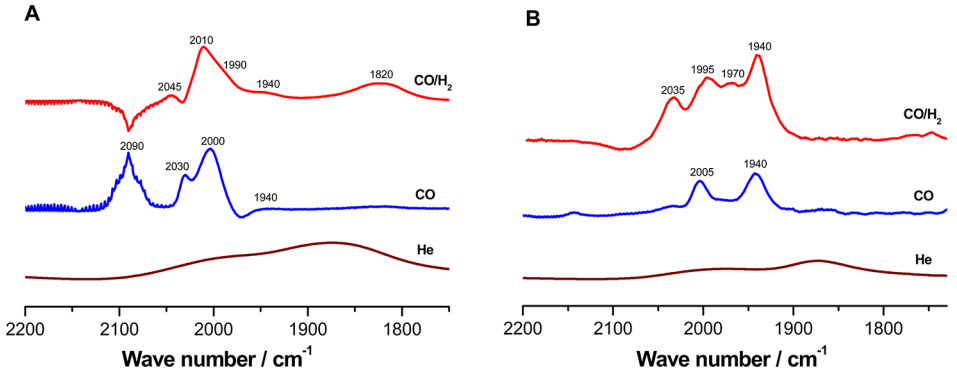

Figure 4. In situ FTIR of (A) PPh_3-Rh/SiO_2 and (B) X-Rh/SiO_2 catalysts in the presence of CO and synthesis gas showing the formation of homogeneous catalysts. L/Rh = 15, Rh = 0.2 wt %, T = 393 K.

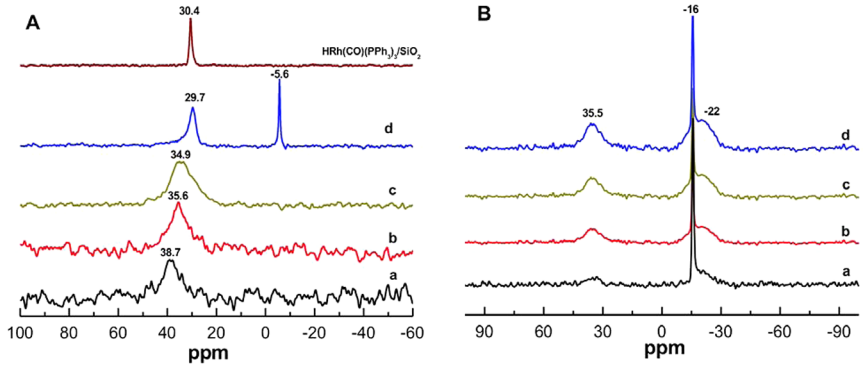

Figure 5. Solid-state ^{31}P MAS NMR spectra of (A) PPh_3-modified Rh/SiO_2 (PPh_3/Rh = 15) and (B) X-modified Rh/SiO_2 (X/Rh = 15) spent catalyst for different Rh weight loadings: Rh = (a) 0.05, (b) 0.2, (c) 0.5, and (d) 1 wt %.

1970 cm^{-1} as well as narrow bands at 2000 and 1940 cm^{-1} (Supporting Information). As the CO partial pressure was increased to 1 atm, the intensity of these bands increased further, with nearly constant relative intensities. The broad peak at 1970 cm^{-1} arises from linear Rh(CO), whereas the bands at 2000 and 1940 cm^{-1} are due to $Rh(CO)_2$ species red-shifted as a result of the presence of adsorbed PPh_3.[20] Coordination of electron-donating PPh_3 ligand enhances the electron density around the rhodium center, resulting in substantial back-donation to CO ligands, thereby lowering the CO vibration frequency. Addition of H_2 to CO in the gas stream resulted in the appearance of bands at 2045, 2010, 1990, and 1950 cm^{-1}. The positions of these bands are identical to those observed for soluble $HRh(CO)_n(PPh_3)_{4-n}$ complexes. The peaks at 2045 and 1990 cm^{-1} are attributable to *ee*-$HRh(CO)_2(PPh_3)_2$, whereas the peaks at 2010 and 1950 cm^{-1} are attributable to *ea*-$HRh(CO)_2(PPh_3)_2$ complexes.[21,22] The band at 1900 cm^{-1} can be assigned to $HRh(CO)(PPh_3)_3$ species downshifted because of the presence of three PPh_3 groups.[21] The growth of bands associated with $HRh(CO)(PPh_3)_3$ and $HRh(CO)_2(PPh_3)_2$ with increasing partial pressure provides evidence for in situ formation of homogeneous catalysts. The nearly linear growth of these bands with increasing synthesis gas pressure also indicates that an equilibrium exists between gaseous CO, Rh metal, and homogeneous $HRh(CO)_n(PPh_3)_{4-n}$ species.[15] Notably, no bands were observed in the region of 1850−1700 cm^{-1}, characteristic of bridging CO ligands, suggesting the absence of dimeric rhodium complexes.

The IR spectra of PPh_3-modified 0.2% Rh/SiO_2 (PPh_3/Rh = 15) differed from those of PPh_3-modified 1% Rh/SiO_2 as a result of the different amounts of PPh_3 ligands (per gram of support) on the silica support. This leads to the formation of PPh_3-rich $HRh(CO)(PPh_3)_3$ homogeneous species in 1 wt % Rh samples; the 0.2% Rh sample leads to ligand-lean $HRh(CO)_3(PPh_3)$ type species. This leads to the difference in the IR spectra of both samples. As seen in Figure 4A, contacting the catalyst with CO in He (1 atm) produced sharp CO bands at 2090, 2030, 2000, and 1940 cm^{-1}. As noted above, the bands at 2000 and 940 cm^{-1} are due to $Rh(CO)_2$ species red-shifted due to the presence of adsorbed PPh_3, whereas the intense bands at 2090 and 2030 cm^{-1} arise from the geminal-dicarbonyl rhodium species. Addition of H_2 to CO in the gas stream produced peaks at 2045, 2010, 1990, and 1940 cm^{-1} associated with $HRh(CO)_2(PPh_3)_2$ species. Remarkably, there is no evidence for phosphine rich $HRh(CO)(PPh_3)_3$ species, as were observed in the spectrum of PPh_3-modified 1% Rh/SiO_2. More interestingly, this catalyst showed the presence of a broad peak at 1820 cm^{-1}, which is characteristic of bridging CO present in rhodium dimers.

IR spectra of bidentate xantphos-modified 0.2% Rh/SiO_2 catalyst (X-Rh/SiO_2, X/Rh = 15) in the presence of synthesis gas are presented in Figure 4B. Upon contacting the catalyst with CO in He, carbonyl bands appeared at 2005 and 1940 cm^{-1}. The positions of these bands are attributed to the formation of the rhodium carbonyl phosphine complexes.[12] Addition of H_2 to CO to the gas stream resulted in the formation of four carbonyl bands at 2035, 1995, 1970, and 1940 cm^{-1}. These features are identical to those observed for Rh complexes formed with xantphos dissolved in organic solvents, ionic liquids, and supported ionic liquid phase (SILP) catalytic systems (Supporting Information).[22] The bands at 2035 and 1970 cm^{-1} are attributable to *ee*-$HRh(CO)_2(X)$, in which both

dx.doi.org/10.1021/cs3007445 | ACS Catal. 2013, 3, 348−357

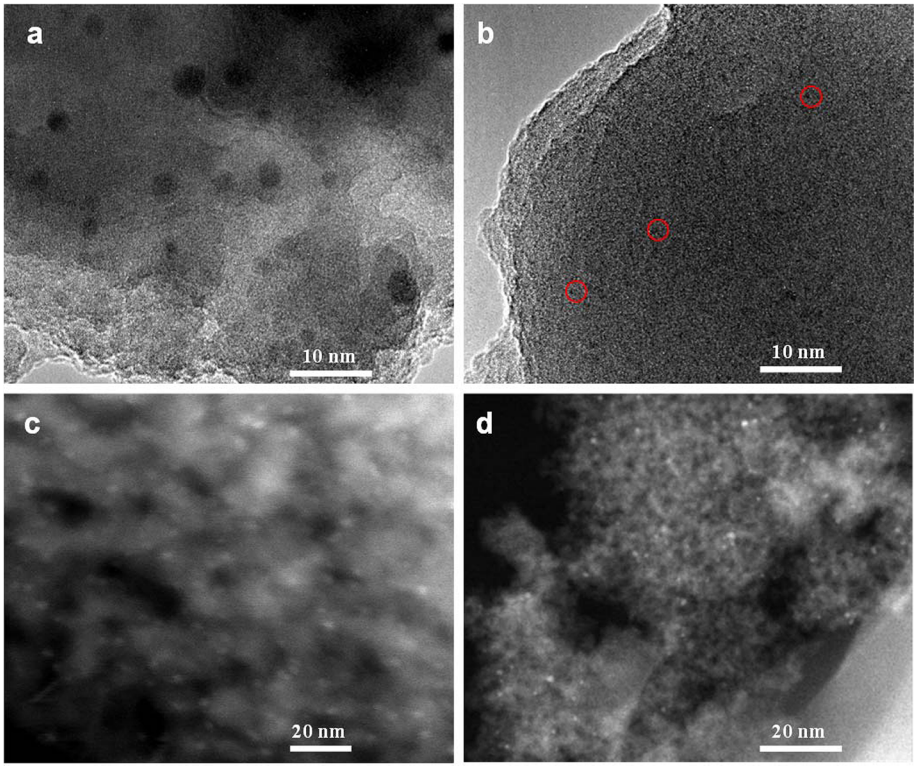

Figure 6. (a, b) High-resolution transmission electron micrographs (HR-TEM) and (c, d) high-angle annular dark field scanning tunneling electron microscopy (HAADF-STEM) of (a, c) 1% Rh/SiO_2 and (b, d) 0.2% Rh/SiO_2 samples. Red circles represent rhodium nanoparticles of ~1 nm diameter.

phosphorus atoms occupy equatorial coordination sites, and the bands at 1995 and 1940 cm^{-1} are attributable to *ea*-$HRh(CO)_2(X)$, in which one phosphorus atom is equatorial and the other is apical. No bands were observed in the region characteristic of CO bridging ligands (1800−1700 cm^{-1}), suggesting the absence of dimeric $[Rh(X)(CO)(\mu\text{-}CO)]_2$ species for catalysts prepared with xantphos ligand on Rh/SiO_2.

3.3.2. ^{31}P MAS NMR Spectroscopy. Further evidence for in situ formation of homogeneous complexes over the phosphine-modified Rh/SiO_2 catalysts was obtained by solid-state ^{31}P MAS NMR spectroscopy. The spectrum of a PPh_3-modified silica support (PPh_3/SiO_2) exhibits a band at −5.6 ppm ascribed to PPh_3 adsorbed on the silica surface.[13] By contrast, PPh_3-Rh/SiO_2 showed the presence of physisorbed phosphine at −5.6 ppm and a broad, less intense, peak centered at 33 ppm due to phosphine adsorbed on rhodium nanoparticles. The position of this peak is similar to the peak observed at 36 ppm in the ^{31}P MAS NMR spectra of $HRh(CO)(PPh_3)_3/SiO_2$, which is attributed to the coordination of the Rh^+ ion and the PPh_3 of the rhodium complex[13] (Supporting Information). Figure 5 shows the ^{31}P MAS NMR spectrum of the spent PPh_3-modified Rh/SiO_2 and the xantphos-modified Rh/SiO_2 catalysts. The spent PPh_3-0.05% Rh/SiO_2 catalyst showed a sharp peak at ~38 ppm, and with increasing rhodium loading, a progressive upfield shift of this band is observed. Free phosphine characterized by a peak at −5.6 ppm was observed in the spent PPh_3-1% Rh/SiO_2 catalyst, whereas free phosphine was absent for catalysts prepared with lower rhodium loadings. This result suggests that PPh_3-1% Rh/SiO_2 contains free phosphines and homogeneous species, mainly as $HRh(CO)(PPh_3)_3$. Indeed, a phosphine-modified $HRh(CO)(PPh_3)_3/SiO_2$ (Rh = 1%) spent catalyst also showed a peak at 30 ppm. By contrast, X-Rh/SiO_2 exhibited peaks at 36, −16, and −22 ppm, similar to the features observed for sulfoxantphos-modified rhodium SILP catalysts.[12] The peak at −16 ppm is attributable to xantphos weakly physisorbed on silica; the broad peak at −22 ppm is attributable to phosphorus atoms in either singly protonated or nonprotonated, strongly physisorbed xantphos ligands. The peak at 35 ppm is assigned to the phosphine groups of xantphos interacting with Rh. These results are indicative of in situ formation of homogeneous $HRh(CO)_n(L)_{4-n}$ species on phosphine-modified Rh/SiO_2.

3.3.3. HR-TEM Measurements. HR-TEM image of 1% Rh/SiO_2 showed rhodium nanoparticles ~5 nm in diameter, whereas the 0.2% Rh/SiO_2 catalyst showed particles 1.5 nm in diameter. In both cases, the particles are well distributed over the support surfaces, as shown in Figure 6. Further confirmation for the high dispersion of rhodium nanoparticles on the silica support surfaces was obtained by the high angle annular dark-field-scanning tunneling electron microscopy (HAADF-STEM). A spent catalyst showed no difference in the size of the rhodium nanoparticle, highlighting that the particle remains unchanged under the reaction conditions.

4. DISCUSSION

The strong similarities in the rate parameters for hydroformylation of propene over phosphine- and xantphos-modified Rh/SiO_2 and the corresponding homogeneous species of the type $HRh(CO)_n(L)_{4-n}$[15] suggest that Rh complexes are produced in situ. The manner in which this occurs is as follows: Nanoparticles of Rh supported on silica or alumina are known to undergo corrosive chemisorption in the presence of CO to produce Rh(I) *gem*-dicarbonyl species ($Rh^{(I)}(CO)_2$) exhibiting bands at 2090 and 2030 cm^{-1}.[20] It has been

dx.doi.org/10.1021/cs3007445 | *ACS Catal.* 2013, 3, 348−357

proposed that such species are formed from supported Rh nanoparticles by the adsorption of CO on the surface of the particle, which leads to a weakening of Rh−Rh bonds due to the higher strength of Rh−CO bonds (185 kJ) than Rh−Rh bonds (44.5 kJ).[23] Neutral Rh dicarbonyl species formed via this process can then interact with the hydroxyl groups of the support to release H_2 and produce $\equiv Si-O-Rh^{(I)}(CO)_2$ species, as shown in Scheme 1. Evidence for the formation of

Scheme 1. Proposed Mechanism for the Formation of Homogenous Catalysts on Phosphine-Modified Rh/SiO_2

$$Rh^{o} + 2\,CO \longrightarrow Rh^{o}(CO)_2$$

$$2\,Rh^{o}(CO)_2 + 2\,Si\text{-}OH \longrightarrow 2\,Si\text{-}O\text{-}Rh^{(I)}(CO)_2 + H_2$$

$$Si\text{-}O\text{-}Rh^{(I)}(CO)_2 + H_2 \longrightarrow HRh^{(I)}(CO)_2 + Si\text{-}OH$$

$$HRh^{(I)}(CO)_2 + 2\,PPh_3 \longrightarrow HRh(CO)_2(PPh_3)_2$$

such species can be drawn from the results of in situ IR spectroscopy. The IR spectra for both 0.2 wt % and 1 wt % Rh/SiO_2 exposed to CO at 120 °C showed bands for *gem*-rhodium dicarbonyl bands at 2090 and 2030 cm^{-1} (Supporting Information) and the concurrent decrease in the intensity of the band at 3660 cm^{-1} due to $\equiv Si-O-H$ vibrations. Interaction of H_2 with the $\equiv SiO-Rh^{(I)}(CO)_2$ species leads to the formation of mobile $HRh(CO)_2$ species and a restoration of hydroxyl groups.[24] We envisage that, under reaction conditions, the phosphine ligands interact with these species to generate in situ $HRh(CO)_2(X)$ species in the presence of xantphos ligand and $HRh(CO)_n(PPh_3)_{4-n}$ species in the presence of PPh_3 (Scheme 1).

The effect of the PPh_3/Rh ratio on the rate of *n*- and isobutanal formation can be attributed to the equilibrium shown in Scheme 2. Because of the low CO partial pressures used, formation of $HRh(CO)_4$ species is unlikely under our experimental conditions, which explains the absence of catalytic activity without PPh_3 ligands. The increase in catalytic activity with increasing PPh_3/Rh ratio is due to an increase in the concentration of $HRh(CO)_n(PPh_3)_{4-n}$ species (Figure 1). The need for excess PPh_3 arises from the relatively weak $Rh-PPh_3$ binding.[25] Hence, to maintain a high activity and regioselectivity, excess PPh_3 is required to drive the equilibrium in favor of $HRh(CO)(PPh_3)_2$. Consequently, as the ligand concentration increases, the equilibria in Scheme 2 shift to the left, and the steric bulk of the complexes increases, contributing to the formation of complexes that produce higher n/iso ratios. Stated another way, the enhancement in linear aldehyde selectivity observed at high PPh_3/Rh ratios may be due to the hydroformylation cycle in which each intermediate contains two phosphines per rhodium derived from $HRh(CO)(PPh_3)_3$. The decreased activity for $PPh_3/Rh > 15$ is related to the difficulty of $HRh(CO)_n(PPh_3)_{4-n}$ 18-electron complexes to lose a PPh_3 ligand to form the 16-electron species or to the formation of $HRh(L)_4$ type species.[15] By contrast, the bidentate xantphos ligand favors the formation of $HRh(CO)_2(X)$ 18-electron species, which then dissociates a CO ligand to form the catalytically active, regioselective, 16-electron HRh(CO)-(X) species.

The dependence of propene hydroformylation activity and stability on rhodium loading can be interpreted in the following manner. It is known that the ratio of surface atoms located at edges and vertices relative to those in planes increases significantly as the size of the nanoparticle becomes small. Our TEM observations show that the size of the Rh particles supported on SiO_2 decreases with decreasing Rh loading. Since the Rh atoms located at the particle corners and edges are more coordinatively unsaturated, they are more susceptible to corrosive chemisorption than Rh atoms located on the planar surfaces of the particles. Thus, we attribute the higher specific activity per Rh site observed with decreasing Rh weight loading to an increase in the facility with which corrosive chemisorption releases Rh atoms from Rh nanoparticles, which in turn increases the concentration of $Rh^{(I)}(CO)_2$ species. Thus, the highly dispersed and smaller nanoparticles (preferably cluster sized) leads to an ease of formation of the homogeneous complexes in the presence of syngas than larger particles. This result is clearly confirmed from the comparison between the size of the rhodium nanoparticles that the highly dispersed and smaller nanoparticles showed a higher rate than the larger Rh nanoparticles (Figure 2).

The higher catalytic activity of bidentate xantphos-modified Rh/SiO_2 compared with monodentate PPh_3-modified Rh/SiO_2 can be related to the chelating ability of xantphos, which yields a higher concentration of the coordinated Rh species.[1] This, in turn, results in increased complexation of the rhodium center by the diphosphine X ligand, and the rigid backbone of the ligand compells the phenyl groups of xantphos to exert a greater degree of steric hindrance on the alkene entering the coordination sphere, favoring linear products. Usage of different ligands suggests that as the electron density on the rhodium atom is reduced by increasing the electron-withdrawing functionality in the phosphine ligand ($3F\text{-}PPh_3\text{-}Rh/SiO_2$ vs $OMe\text{-}PPh_3\text{-}Rh/SiO_2$), the selectivity to linear aldehydes increased with a significant change in the activity. Since para-substituted aryl phosphines were utilized in the present study, the steric environment around the active rhodium center is nearly constant.[16] Hence, the catalytic activity differences can be correlated nicely with the electronic properties of the

Scheme 2. Illustration of Species That Might Form $HRh(CO)_2(PPh_3)_2$ under Reaction Conditions

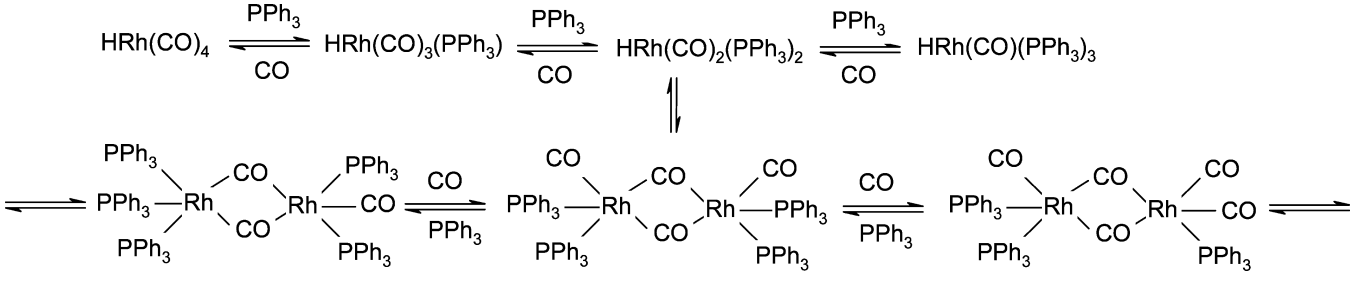

dx.doi.org/10.1021/cs3007445 | ACS Catal. 2013, 3, 348−357

phosphine ligands. If the ligand has good back-bonding ability, the equilibrium in Scheme 2 will shift to the left to favor $HRh(CO)(L)_3$ to prevent excess charge building up on $Rh^{(I)}$ cations. These results suggest that electron-withdrawing phosphine ligands tend to form the 18-electron $HRh(CO)_n(PPh_3)_{4-n}$ species and then rapidly lose a ligand to form the coordinatively unsaturated, active 16-electron $HRh(CO)_n(PPh_3)_{3-n}$ species. Consistent with this interpretation, electron-withdrawing substituents in phosphine ligands increase the carbonyl stretching frequencies, which provide direct evidence that the M-CO bond is weakened as the electron withdrawing ligands reduce M−CO $d\pi-p\pi$ interactions.[16] The low *n*-aldehyde selectivity observed with the phosphite ligands suggests that the electronegativity difference of the groups attached to the phosphorus will change the σ donor and π acceptor properties of the ligands, leading to a change in the overall performance of the catalysts.[25]

The catalytic activity, n/iso ratio, and stability of phosphine-modified Rh/SiO_2 (PPh_3-Rh/SiO_2) and $HRh(CO)(PPh_3)_3/SiO_2$ differ significantly. Phosphine-modified Rh/SiO_2 is stable under reaction conditions, whereas $HRh(CO)(PPh_3)_3/SiO_2$ progressively loses activity under identical reaction conditions (Supporting Information). These observations suggest that the interaction of the Rh complex with the rest of the catalyst is different in the two samples. As discussed earlier, we envisage that the formation of geminal rhodium dicarbonyl species provides a favorable stabilizing effect, as proposed by Augustine and co-workers using heteropolyacid as linkers (Scheme 3).[26]

Scheme 3. Proposed Stabilization of $HRh(CO)_n(PPh_3)_{4-n}$ on Rh/SiO_2

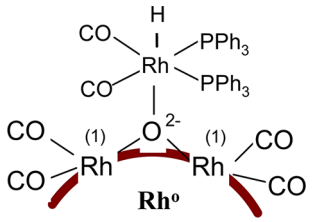

Comparison of the IR spectra of PPh_3-Rh/SiO_2 and $HRh(CO)(PPh_3)_3/SiO_2$ shows a greater red shift (~1945 cm^{-1}) for the CO resonances of homogeneous species in PPh_3-Rh/SiO_2 than the Wilkinson-catalyst-supported silica sample (~1975 cm^{-1}) (see Supporting Information). The sharp decrease in activity of the $HRh(CO)(PPh_3)_3/SiO_2$ catalyst thus relates to the weak interaction of the homogeneous catalyst with the silica surface and thereby to the easy formation of inactive dimers/clusters.[12,13]

The kinetics of butanal formation observed for monodentate PPh_3-modified and bidentate xantphos-modified Rh/SiO_2 catalysts can be interpreted using the mechanism proposed by Heck and Breslow.[27] $HRh(CO)(PPh_3)_3$ (**A**) and $HRh(CO)_2(PPh_3)_2$ (**B**) species exist in equilibrium for phosphine-modified PPh_3-Rh/SiO_2 catalysts, and hydroformylation is initiated with the loss of a CO ligand to form the 16-electron species, $HRh(CO)(PPh_3)_2$ (**C**) (Scheme 4A). Propene then coordinates to species **C** to form a η^2-Rh complex (species **D**). Migratory insertion into the Rh−H bond forms a propyl-Rh complex (species **E**). CO then adds to species **E** to form an 18-electron intermediate species **F**. Migratory insertion of the propyl to a carbonyl group leads to the formation of an acyl intermediate (species **G**). Oxidative addition of H_2 forms the 18-electron Rh(III) species **H**, followed by the reductive elimination of butanal. For X-Rh/SiO_2 catalysts, hydroformylation of propene is initiated by the loss of a CO ligand from $HRh(CO)_2(X)$ (species **A**) to form the 16-electron species HRh(CO)(X) (**B**) (Scheme 4B). Isobutanal is formed in a catalytic cycle by an analogous mechanism, in which species **D**−**G** involve a secondary, rather than a primary, alkyl species.

The observed reaction orders at 363 K for PPh_3-Rh/SiO_2 catalyst were first order in C_3H_6, CO and H_2, suggesting that the rate-determining step (RDS) is the oxidative addition of hydrogen. Under this assumption, the rate of butanal formation can be written as follows:

$$r_{\text{butanal}} = \frac{\prod_{i=1}^{6} K_i k_7 P_{C_3H_6} P_{CO} P_{H_2} / [PPh_3]}{1 + K_1 P_{CO} / [PPh_3]} [Rh] \quad (1)$$

where k_i is the rate coefficient for reaction *i*, K_i is the equilibrium constant for reaction *i*, P_j is the partial pressure of species *j*, $[PPh_3]$ is the concentration of PPh_3 species, and [Rh] is the total moles of Rh. If it is assumed that the second term in the denominator of eq 1 is small relative to unity, then the rate expression is consistent with the observed kinetics at 363 K. Similar positive order kinetics have been reported earlier for hydroformylation reactions carried out at pressures lower than those described as typical hydroformylation conditions (343−393 K, 10−30 atm).[15,28]

The apparent reaction orders observed at 363 K for xantphos-modified Rh/SiO_2 catalyst were first-order in propene, negative-order in CO, and nearly zero-order in H_2. These results suggest that the rate-determining step (RDS) now becomes alkene insertion, in good accordance with the kinetics reported for hydroformylation over sulfoxantphos-containing Rh-SILP catalysts.[19] Further support for alkene insertion as the RDS for diphosphine ligands can be drawn from the work of van Leeuwen and co-workers.[29] Upon the basis of the hydroformylation reaction mechanism and considering alkene insertion to be the irreversible, rate-limiting step, the rate of butanal formation is given by the following relation:

$$r_{\text{butanal}} = \frac{K_1 K_2 k_3 P_{C_3H_6} [Rh]}{P_{CO} + K_1 + K_1 K_2 P_{C_3H_6}} \quad (2)$$

where k_i is the rate coefficient for reaction *i*, K_i is the equilibrium constant for reaction *i*, P_j is the partial pressure of species *j*, and [Rh] is the total moles of Rh.

Equation 2 is consistent with the observed kinetics at 363 K. The rate of butanal synthesis is zero-order in the partial pressure of H_2 and less than first-order in the partial pressure of C_3H_6. As the partial pressure of C_3H_6 increases, the $K_1K_2P_{C_3H_6}$ term in the denominator becomes increasingly significant, thereby reducing the effective order from unity. The experimentally observed, inhibitory effect of CO is also effectively represented by eq 2. Since the order of CO is −0.4, the remaining terms in the denominator are significant in magnitude compared with P_{CO}.

The decrease in the n/iso ratio from low temperature to high temperature over the phosphine-modified Rh/SiO_2 catalysts can be explained as follows: PPh_3-Rh/SiO_2 catalysts show a very high n/iso ratio of 22 at 353 K, which decreases to 3 at 413 K. Preference for forming linear versus branched aldehydes in PPh_3-Rh/SiO_2 catalysts can be attributed to the preferred

dx.doi.org/10.1021/cs3007445 | ACS Catal. 2013, 3, 348−357

Scheme 4. Proposed Mechanism for the Hydroformylation of Propene on (i) PPh_3-Rh/SiO_2 and (ii) X-Rh/SiO_2

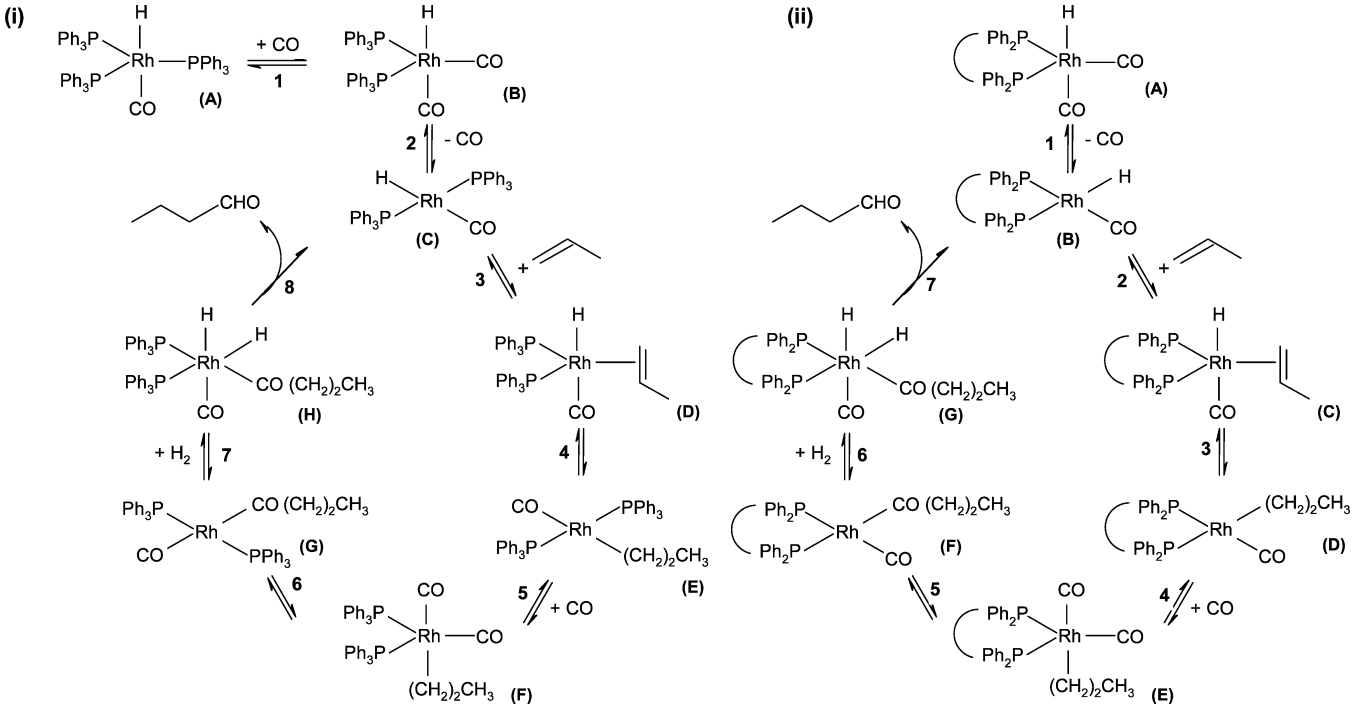

isomerization of $HRh(CO)(PPh_3)_2$ to the structure in which both phosphine groups are coordinated in the equatorial plane.[15] The high n/iso ratio observed with PPh_3-Rh/SiO_2 at low temperatures is consistent with studies conducted with $HRh(CO)(PPh_3)_3$ in homogeneous solutions. For X-Rh/SiO_2 catalysts, a decrease in the n/iso molar ratio from 15 at 353 K to ~8 at 413 K was observed. For the bidentate xantphos ligand, the regioselectivity is determined by alkene insertion into the Rh−H bond to form either primary or secondary alkyls.[1] The apparent activation energies measured for *n*- and isobutanal formation are 65 and 75 kJ mol^{-1}, respectively. Therefore, the resulting n/iso ratio is high because primary alkyls are favored kinetically over secondary alkyls. Indeed, theoretical studies demonstrate that the transition for the formation of secondary alkyls is ~9 kJ mol^{-1} greater than that for the formation of primary alkyls because of the steric effects exerted from the phenyl groups of the phosphine ligand.[30] The decrease in the n/iso ratio at high temperature is due to a shift from the thermodynamically favorable primary alkyl complex to the less favorable secondary alkyl complex. These results are in agreement with previous deuteroformylation studies, which found that Rh−alkyl formation is irreversible at low temperature but reversible at higher temperatures.[19,31]

5. CONCLUSIONS

The results of this study provide a detailed understanding of the factors influencing the activity, selectivity, and stability of phosphine-modified Rh/SiO_2 catalysts for the hydroformylation of propene. Catalyst performance and stability are found to be strong functions of the nature and concentration of ligand and rhodium loading. The catalysts produced are very stable and exhibit 100% selectivity to butyraldehydes; no propane or alcohols were detected. Higher catalytic activity and n/iso ratios were observed over xantphos-modified Rh/SiO_2 than over phosphine-modified Rh/SiO_2. The reaction temperature has a strong effect on the activity and regioselectivity of PPh_3-Rh/SiO_2. A first-order dependence on the partial pressures of propene, CO, and H_2 were observed for PPh_3-Rh/SiO_2, whereas X-Rh/SiO_2 catalysts showed first-order partial pressure dependence in propene, negative order in CO, and zero order in H_2. Differences in the kinetics between the monodentate and the bidentate phosphine ligands are related to the difference in the rate-limiting steps. Oxidative addition of hydrogen is the rate-limiting step for PPh_3-Rh/SiO_2, whereas alkene insertion is the rate-limiting step over the X-Rh/SiO_2. In situ FTIR and ^{31}P MAS NMR indicate the in situ formation of $HRh(CO)_2(X)$ species on the xantphos-modified Rh/SiO_2 catalyst and $HRh(CO)_n(PPh_3)_{4-n}$ species on the phosphine-modified Rh/SiO_2. In each case, isolated $Rh^{(I)}(CO)_2$ species are produced via corrosive chemisorption, as shown in Scheme 1.

■ ASSOCIATED CONTENT

Supporting Information

Seventeen figures are provided as Supporting Information. This material is available free of charge via the Internet at http://pubs.acs.org.

■ AUTHOR INFORMATION

Corresponding Author

*Tel. +1 510 642 1536. Fax +1 510 642 477. E-mail: bell@cchem.berkeley.edu.

Notes

The authors declare no competing financial interest.

■ ACKNOWLEDGMENTS

This work was supported by the XC2 program funded by BP. The authors thank Dr. Chris Canlas (Berkeley NMR facility) for his assistance in acquiring the NMR spectra, Eric Bloch for the TGA results, Dr. Zhengmeng Peng for the HR-TEM results.

REFERENCES

(1) *Rhodium Catalyzed Hydroformylation*; van Leeuwen, P. W. N. M., Claver, C., Eds.; Kluwer, Dordrecht, 2000.
(2) Cornils, B.; Hermann, W. A.; Rasch, M. *Angew. Chem., Int. Ed.* **1994**, *33*, 2144−2163.
(3) Cole-Hamilton, D. J. *Science* **2003**, *299*, 1702−1706.
(4) Beller, M.; Cornils, B.; Frohning, C. D.; Kohlpainter, C. W. *J. Mol. Catal. A: Chem.* **1995**, *104*, 17−85.
(5) Sandee, A. J.; Reek, J. N. H.; Kamer, P. C. J.; van Leeuwen, P. W. N. M. *J. Am. Chem. Soc.* **2001**, *123*, 8468−8476.
(6) Mehnert, C. P.; Cook, R. A.; Dispenziere, N. C.; Afeworki, M. *J. Am. Chem. Soc.* **2002**, *124*, 12932−12933.
(7) Arhanchet, J. P.; Davis, M. E.; Hanson, B. E. *J. Catal.* **1991**, *129*, 94−99.
(8) Riisager, A.; Wasserscheid, P.; Van Hal, R.; Fehrmann, R. *J. Catal.* **2003**, *219*, 452−455.
(9) Riisager, A.; Fehrmann, R.; Flicker, S.; van Hal, R.; Haumann, M.; Wasserscheid, P. *Angew. Chem., Int. Ed.* **2005**, *44*, 815−819.
(10) Riisager, A.; Fehrmann, R.; Haumann, M.; Gorle, B. S. F.; Wasserscheid, P. *Ind. Eng. Chem. Res.* **2005**, *44*, 9853−9859.
(11) Riisager, A.; Fehrmann, R.; Haumann, M.; Wasserscheid, P. *Eur. J. Inorg. Chem.* **2006**, 695−706.
(12) Shylesh, S.; Hanna, D.; Werner, S.; Bell, A. T. *ACS Catal.* **2012**, *2*, 487−493.
(13) Yan, L.; Ding, Y. J.; Zhu, H. J.; Xiong, J. M.; Wang, T.; Pan, Z. D.; Lin, L. W. *J. Mol. Catal. A: Chem.* **2005**, *234*, 1−7.
(14) Zhu, H. J.; Ding, Y. J.; Yan, L.; Xiong, J. M.; Lu, Y.; Lin, L. W. *Catal. Today* **2004**, *93*, 389−393.
(15) Kim, T. J.; Celik, F. E.; Hanna, D. G.; Shylesh, S.; Werner, S.; Bell, A. T. *Top. Catal.* **2011**, *54*, 299−305.
(16) Moser, W. R.; Papile, C. J.; Brannon, D. A.; Duwell, R. A. *J. Mol. Catal.* **1987**, *41*, 271−292.
(17) Sandee, A. J.; Slagt, V. F.; Reek, J. N. H.; Kamer, P. C. J.; van Leeuwen, P. W. N. M. *Chem. Commun.* **1999**, 1633−1634.
(18) Dupont, J.; Silva, S. M.; De Souza, R. F. *Catal. Lett.* **2001**, *77*, 131−133.
(19) Hanna, D.; Shylesh, S.; Werner, S.; Bell, A. T. *J. Catal.* **2012**, *292*, 166−172.
(20) Yang, A. C.; Garland, C. W. *J. Phys. Chem.* **1957**, *61*, 1504−1512.
(21) Evans, D.; Yagupsky, G.; Wilkinson, G. *J. Chem. Soc.* **1968**, 2660−2663.
(22) Silvia, S. M.; Bronger, R. P. J.; Freixa, Z.; Dupont, J.; van Leeuwen, P. W. N. M. *New J. Chem.* **2003**, *27*, 1294−1296.
(23) Vant Blik, H. F. J.; Van Zon, J. B. A. D.; Huizinga, T.; Vis, J. C.; Koningsberger, D. C.; Prins, R. *J. Am. Chem. Soc.* **1985**, *107*, 3139−3145.
(24) Basu, P.; Panayotov, D.; Yates, J. T., Jr. *J. Am. Chem. Soc.* **1988**, *110*, 2074−2081.
(25) Pruett, R. L.; Smith, J. A. *J. Org. Chem.* **1969**, *34*, 327−330.
(26) Augustine, R.; Tanielyan, S.; Anderson, S.; Yang, H. *Chem. Commun.* **1999**, 1257−1258.
(27) Heck, R. F.; Breslow, D. S. *J. Am. Chem. Soc.* **1962**, *84*, 2499−2503.
(28) Deshpande, R. M.; Bhanage, B. M.; Kanagasabapathy, S.; Chaudhari, R. V. *Ind. Eng. Chem. Res.* **1998**, *37*, 2391−2396.
(29) Zuidema, E.; Escorihuela, L.; Eichelsheim, T.; Carbo, J. J.; Bo, C.; Kamer, P. C. J.; van Leeuwen, P. W. N. M. *Chem.—Eur. J.* **2008**, *14*, 1843−1851.
(30) Carbo, J.; Maseras, F.; Bo, C.; van Leeuwen, P. W. N. M. *J. Am. Chem. Soc.* **2011**, *123*, 7630−7638.
(31) Casey, C. P.; Petrovich, L. M. *J. Am. Chem. Soc.* **1995**, *117*, 6007−6013.